LA-10744

LA--10744

DE87 000806

UC-37
Issued: September 1986

A High-Temperature Quadrupole Mass Spectrometer for Studying Vaporization from Materials Heated by a CO_2 Laser

Leif Fredin*
George P. Hansen*
Madeline P. Sampson*
John L. Margrave*
Robert G. Behrens

DISCLAIMER

*Department of Chemistry, Rice University, Houston, TX 77001

Los Alamos National Laboratory
Los Alamos, New Mexico 87545

A HIGH-TEMPERATURE QUADRUPOLE MASS SPECTROMETER FOR STUDYING VAPORIZATION FROM MATERIALS HEATED BY A CO_2 LASER

by

Leif Fredin, George P. Hansen, Madeline P. Sampson,
John L. Margrave, and Robert G. Behrens

ABSTRACT

To evaluate the effectiveness of mass spectrometry techniques in studying vaporization from selected materials, we designed a mass spectrometer that can be used either with a continuous wave or pulsed laser heating system or with a conventional furnace heating system. Our experimental apparatus, the components of which are described in detail, consisted of a quadrupole mass spectrometer positioned in a crossed-beam configuration, controlling electronics, a data acquisition system, a vacuum system, a cryogenic collimation system, and a laser heating system. Results of mass spectral scans taken during laser pyrolysis of polymeric materials and laser vaporization of graphite were compatible with data reported in other studies. Results of mass spectral studies of laser-induced combustion in the Ti + C system are also presented.

I. INTRODUCTION

Scientists have used mass spectrometry with lasers in various configurations to study processes such as laser-induced pyrolysis, ablation, desorption, and ionization of materials ranging from biological specimens and synthetic polymers to fossil fuels and refractory metals and compounds.[1-3] The primary advantage of a laser heating system—rapid, local heating—is well known. Most of the laser/mass spectrometer systems developed over the past 15 years have been pulsed systems; that is, either the laser and the mass spectrometer together or each separately forms the pulsed part of the system. A pulsed laser is employed when high laser intensities (greater than 10^5 W/cm^2) are required.

However, unlike a pulsed laser, a continuous wave (cw) laser allows steady-state heating; and a continuous-scanning mass spectrometer allows real-time monitoring of volatilization caused by laser heating. Two such systems,[4,5] previously developed, used a cw CO_2 laser operating on the 10.6-μm line as the heat source and a quadrupole mass spectrometer as the monitoring device. The laser beam and the quadrupole axes were situated 90° apart, and each was located 45° from the sample surface.

The systems developed to date have avoided using "head-on" laser vaporization. That is, the laser beam does not impinge normal to the sample surface, and the mass spectrometer does not sample species emitted coincidental to the laser beam axis. Should the laser interact with desorbed species, allowing single- or multiphoton fragmentation and ionization to occur in the desorption plume, the picture of laser/surface processes would be distorted. On the other hand, if the laser beam, the sample, and the mass spectrometer are not coaxial, the ion signal from this configuration is always smaller than the ion signal from samples situated perpendicular to the laser-heated surface. As a crater forms and deepens into the surface, this effect becomes more pronounced, that is, the intensity of the mass spectrometer signal decreases. If the laser intensity is low enough and the wavelength long enough, the importance of multiphoton fragmentation processes occurring is diminished.

Use of a cw laser system in the apparatus described here allows easy comparison of steady-state heating by a laser with heating by classical methods. Including a pulsed CO_2 laser facilitates study of the effects of nonequilibrium heating of solids. We included "head-on" laser heating as an option in the apparatus to allow monitoring of maximum signal intensity throughout various heating experiments.

Unlike earlier designs, the present system uses a set of cryogenically cooled copper baffles to collimate the vapor plume emitted from the heated sample. This feature combined with differential ultrahigh vacuum (UHV) pumping presents a number of significant advantages in data acquisition and processing over a chopped or pulsed system. First, the speed at which data are acquired is limited only by the length of the quadrupole cycle time and the computer system. Second, the cold baffles allow detection of only those species originating on the laser beam axis. The baffles define the molecular beam that enters the ionizer whereas secondary ions and molecules that remain in the vacuum system for a period of time are eventually pumped out without having been detected. Furthermore, the cryogenic baffle system suppresses a skewing of the amount of condensible versus noncondensible vapor species sampled by the mass spectrometer. Finally, the cryogenic baffles substantially reduce the background in the vacuum system surrounding the ionizer. Since samples heated to several thousand degrees outgas large volumes of material, the system design also includes a differential pumping scheme.

II. OVERVIEW OF THE APPARATUS

Figure 1 is a general schematic of the mass spectrometer system. A set of three cryogenically cooled copper baffles (D, E, and F) are positioned between the sample (S) and the electron impact ionization source (J) of the quadrupole mass spectrometer. Orifices drilled in all three baffles and the shields (G and H) share a common axis (X) with the sample and the ionization source. The baffle system, which is in thermal contact with the heat exchanger of a helium displex

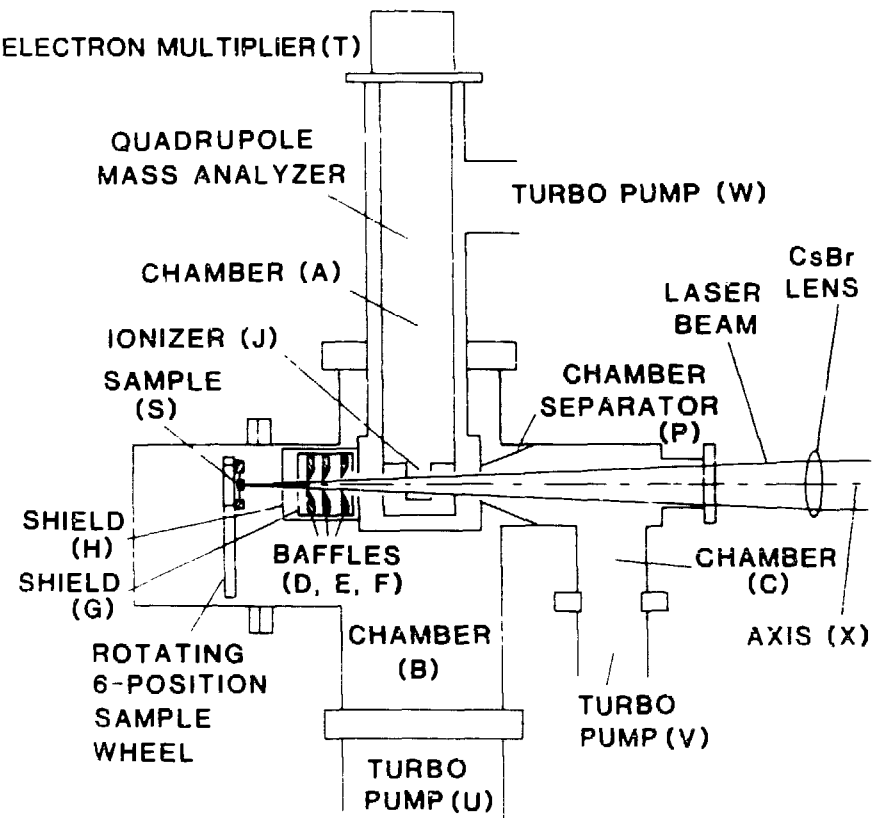

Fig. 1. The mass spectrometer system, including the vacuum chamber network, the cryogenic molecular beam forming system, and the quadrupole mass analyzer.

refrigerator, collimates gaseous species emitted from the front surface of the sample. The neutral molecular beam emitted from the sample surface passes through the ionization region of the mass spectrometer. All gaseous species that do not pass through the baffle orifices are either condensed on the baffles or pumped from the system. The molecular beam diameter in the ionizer is approximately 3 mm. The beam flux is a function of the material being vaporized and the laser power.

The mass spectrometer is positioned in a crossed-beam configuration. Ionized vapor species are deflected into the ion optics region of the ion source, where they are focused by a series of electrostatic lenses. Subsequently, the quadrupole system mass-filters the ions, and an electron multiplier (D) detects them. The portion of the molecular beam not ionized enters a chamber (C) from which it is pumped out of the system. Three turbo pumps (U, V, and W) maintain the system pressure between 10^{-7} and 10^{-9} torr. They are pumped by two dual-stage, rotary-vane pumps.

The present system accommodates either laser heating or resistive furnace heating of the sample. For laser heating, a focused CO_2 laser enters the vacuum system, passes through the ionization region of the mass spectrometer and collimating baffles, and impinges on the sample. Alternatively, the sample may be mounted in the throat of a resistively heated furnace that is aligned coaxially with the collimating-baffles and ionizer. Also, laser and furnace can be used simultaneously to heat the sample.

The photograph of Fig. 2 shows an external view of the apparatus with the vacuum chamber system at center left. The vacuum pumps and cryogenic refrigerator are housed in the cabinet below the vacuum chambers. The controlling electronics for the mass spectrometer, the turbo pumps, and the pressure gauges are located in the rack shown at center right. An electronic data acquisition system is located to the lower right of the rack, just outside the photograph boundaries. The CO_2 laser systems (one cw and the other pulsed) are located behind the rack and the data acquisition system.

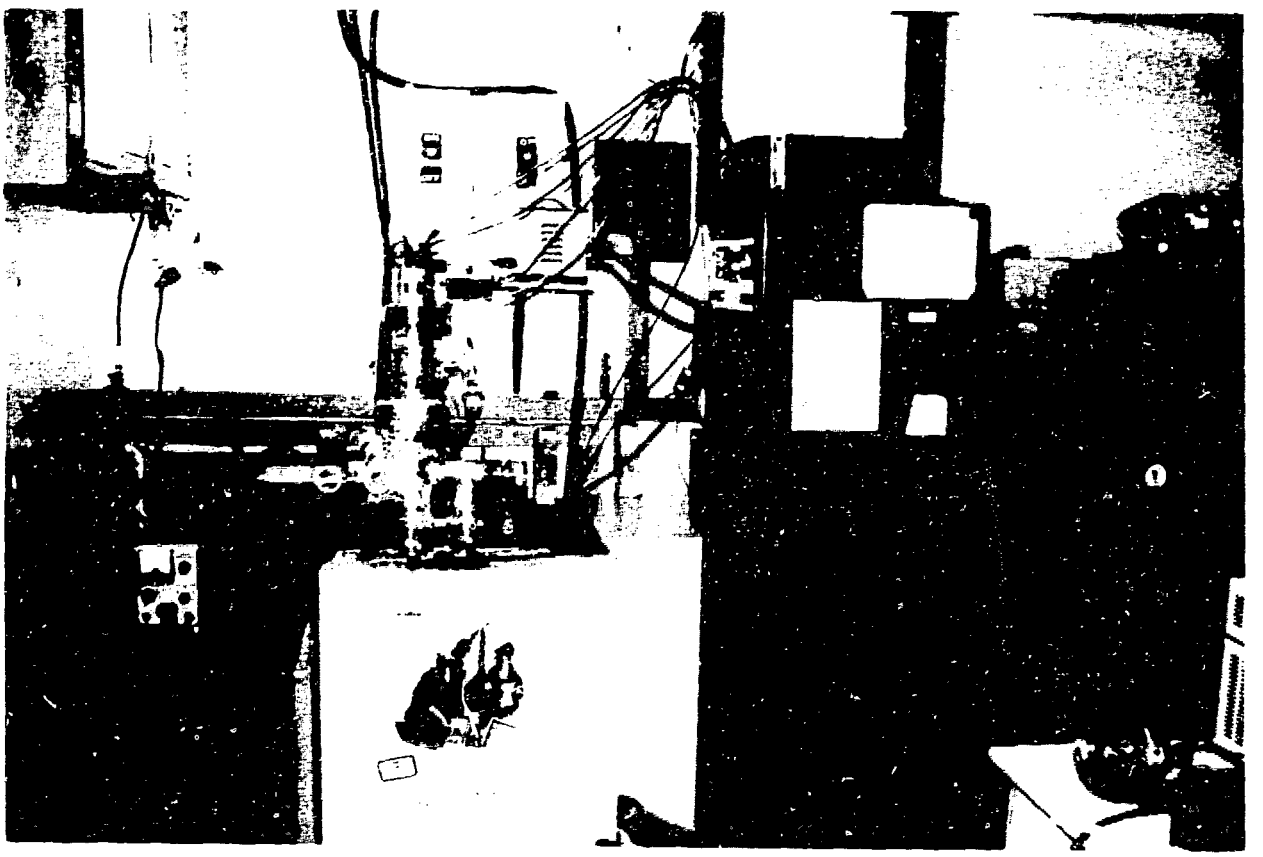

Fig. 2. External view of the mass spectrometer system, including the mass analyzer, controlling electronics, computer, and laser system.

III. DETAILS OF THE APPARATUS

A. The Quadrupole Mass Spectrometer

Figure 3 is a schematic of the quadrupole mass spectrometer, the associated controlling electronics, and the data acquisition system. Digital Equipment Corporation (DEC) manufactured the data acquisition system, and Extranuclear Laboratories, Inc., manufactured the components of the mass spectrometer.

The electron impact ionizer (Extranuclear model number 041-1) was adapted for use in the crossed-beam configuration. It consists of two filaments (one located on each side of and in the same plane as the molecular beam axis), an extractor, one plate lens, and two einzel lenses. The ionizer has a grounded electrostatic lens field separator (ELFS) at the entrance to the quadrupole mass filter to inhibit interference between the fields of the ionizer and the mass filter. The ionizer system is driven by an Electron Energy and Emission Control unit (Extranuclear model number 021-1) and an Ion Energy and Focus Control unit (Extranuclear model number 022-1). The emission current is variable between 100 μA and 50 mA, and the electron energy is variable between 0 and 100 eV. Typically, the ionizing current is set at 2 mA and the electron energy at 70 eV.

The mass filter consists of an ELFS quadrupole (Extranuclear model number 4-162-8) aligned coaxially with the ionizer. The quadrupole consists of four stainless steel rods (20 cm long and 0.95 cm in diameter) spaced such that the diameter of the circle inscribed by the rods is 0.411 cm. The filter will transmit ions with masses in the range 0 to 1400 amu. An Extranuclear QPS power supply drives the quadrupole. This power supply is divided electronically and physically into the following units: (1) a 1.5- to 6-MHz radio frequency power source, (2) a model C, high-Q tuned transformer (High-Q head), and (3) a quadrupole control unit. A sawtooth sweep generated either by an oscilloscope (Tektronix model number 7603) or by a digital-to-analog converter in the DEC PDP 11/03 computer drives the quadrupole control unit. The Model C High-Q head allows an available mass range of 0 to 200 amu. For any given mass range, the scan frequency is variable between 0.1 and 10 Hz. The scan frequency is normally set at 1 Hz or higher.

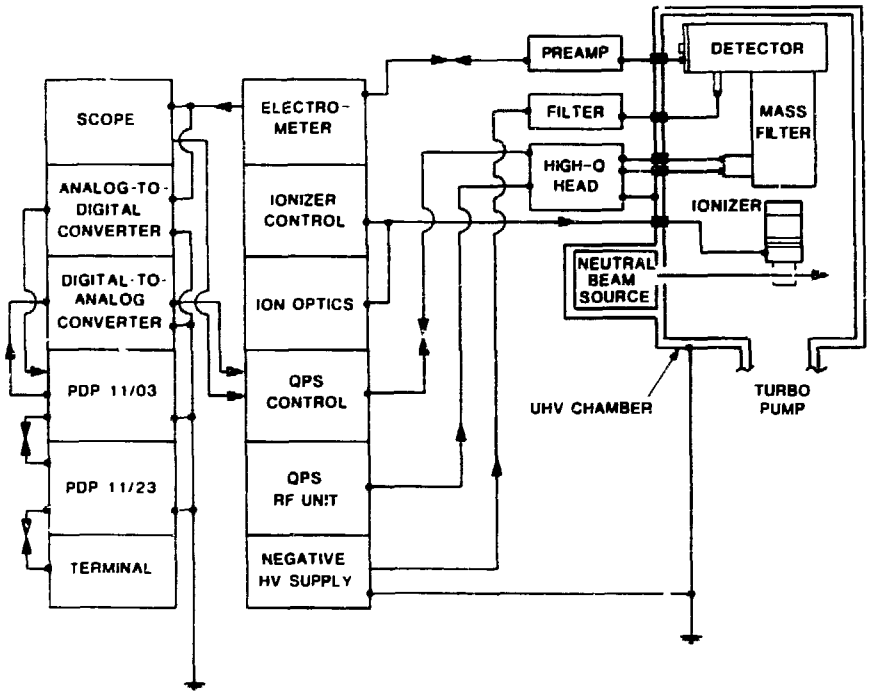

Fig. 3. The mass spectrometer system, controlling electronics, and data acquisition system.

The ion detector is a tandem Faraday plate and a glass analog channeltron electron multiplier (Galileo Electro-Optics type 4816). The maximum initial gain of the electron multiplier is greater than 10^7 at the maximum operating voltage (-3.0 kV). The background count rate of the multiplier is approximately 1 CPS, and the maximum output current is greater than 10^{-6} A. A typical operating potential is between -1.5 and -1.7 kV. The source of the negative high voltage for the electron multiplier is a KEPCO PBX power supply. The output signal from the electron multiplier is initially amplified by a preamp head (Extranuclear model number 032-5) and then further amplified by an electrometer, whose output then goes to an oscilloscope and an analog-to-digital converter in the PDP 11/03 computer.

B. The Data Acquisition System

An Extranuclear Laboratories data acquisition system (model number EL750) acquires the mass spectra. This dual-processor system employs DEC hardware. A DEC PDP 11/03 front-end computer controls the mass spectrometer. This computer sends the signal to ramp the quadrupole for scanning, reads the ion intensities, and transmits the mass-vs-intensity data to the host computer. It may also control the mode of ionization and the operation of solenoid valves. The system's software provides for these peripheral control operations although its hardware currently supports only control of the quadrupole. A PDP 11/23, equipped with an RSX-11M operating system, serves as the host computer for the PDP 11/03. The PDP 11/23 receives information from the operator regarding scan parameters, sends the information to the PDP 11/03, processes and stores the scan data sent from the PDP 11/03, and runs the data manipulation and graphics programs. All of the mass spectrometer programs run on the PDP 11/23 are written in FORTRAN and/or MACRO-11.

The interface between the quadrupole and the PDP 11/03 includes a 16-bit digital-to-analog converter (DAC), a 12-bit analog-to-digital converter (ADC), and a fast electrometer. The DAC is a Hybrid Systems unit (model number 9331-16-6) with a 2-μs settling time. Extranuclear Laboratories makes the electrometer (model number 031-3), whose frequency response is dependent upon the 3-db-point input resistor: dc to 200 kHz (10^5 ohm), dc to 2 kHz (10^7 ohm), or dc to 20 Hz (10^9 ohm). The ADC (Analog Devices model number AD363) has a throughput rate of 30 kHz.

Hardware in this system also includes a Data Systems design 20-megabyte Winchester/1-megabyte floppy-disk-drive storage system (model number 880x/20), a DEC VT-100 terminal with Retro-Graphics enhancement, and a Texas Instruments 810 printer serially interfaced to the terminal via a DEC VT51-PI.

The software in this system consists of the following programs: LOADXB, MSFE, MSTST, MSCAL, MSIN, MSSIM, MSOUT, and SPMTCH. Program LOADXB loads the DRV11-B (an LSI-11-bus-compatible input/output interface) loader into the PDP 11/03 computer. Program MSFE provides the front-end driver and communication routines and default values for various parameters. Several different versions of MSFE provided with the system permit the selection of different scan rates. Both LOADXB and MSFE are continuously running tasks, whereas the operator selects the remaining programs as required.

Program MSTST provides the software diagnostics for evaluating the mass spectrometer/computer interface. In addition, this program permits the evaluation of ion peak shapes and spectrum linearity. Program MSCAL contains standard routines for mass spectrometer calibration. Programs MSIN and MSSIM are data acquisition programs with foreground/background capabilities. These programs support the processing of all data files (including those currently being acquired) during acquisition and provide a real-time display of the total ion current of data currently being acquired. Program MSIN allows acquisition of normal mass spectra within a mass range specified by the operator, and program MSSIM allows acquisition of selected ion data (up to ten sets of eight ions as a function of time). Program MSOUT, the data processing program, performs the following functions: spectrum averaging, background subtraction, mass spectrometry data displayed/plotted in a bar graph format normalized to any ion, mass spectrometry data displayed/plotted as a tabular list, total ion current and individual ion intensities displayed/plotted as a function of scan number or time within user-defined ranges, and integration of chromatographic data.

The data acquisition software also includes a library search program, SPMTCH, which uses a forward library search to compare spectra stored in MSOUT with spectra from the complete EPA/NIH Spectral Data Base. Only the ten best fits to the Spectral Data Base are output for each spectrum tested. At present, we do not have the spectral data base incorporated into our system.

C. The Vacuum System

Figure 1 shows the relative positions of the three turbo molecular pumps (TMPs) and the vacuum chambers. A 0.5-μm, 100-ℓ/min precision vacuum pump (GCA model number DD-100) simultaneously pumps two 40-ℓ/s turbo pumps (Balzers model number TPU-040), shown as (V) and (W) in Fig. 1. A 0.1-μm, 195-ℓ/min precision vacuum pump (GCA model number DD-195) pumps a 170-ℓ/s turbo pump (Balzers model number TPU-170), shown as (U) in Figs. 1 and 4. Two power supplies (Balzers model number TCP-040) drive the 40-ℓ/s pumps, and another power supply (Balzers model number TCP-300) drives the 170-ℓ/s pump. The nominal operating pressure in chambers (A) and (B) is 10^{-9} torr. The pressure in chamber (C) is nominally 10^{-8} torr. Electronically controlled vent valves on each turbo pump allow backfilling of the system to atmospheric pressure with helium.

All vacuum chambers are constructed of stainless steel and have a wall thickness of 1.6 mm. Most flanges are MDC Conflats, which use copper sealing gaskets; however the flange between chamber (B) and the sample chamber uses a Viton Conflat gasket, and the flanges holding NaCl windows use Viton o-rings. The internal volume of the vacuum system is approximately 5 ℓ.

The external walls of the vacuum system are wrapped with seven 600-W heating strips and aluminum foil, and the turbo pumps are equipped with 250-W internal heaters, which expedite outgassing of the internal chamber walls. Separate copper-constantan thermocouples monitor the external temperatures of chambers (A), (B), and (C) as well as the sample chamber. Typically, the system temperature during outgassing is 200°C. The mass spectrometer may serve as a residual gas analyzer during the outgassing procedure.

Figure 4 (see section D for details) shows gate valves (K and Q) on each side of the ionization region of the mass spectrometer. When valve (Q) is closed, chamber (B) can be opened to atmospheric pressure while chambers (A) and (C) remain at 10^{-9} torr. When both gate valves are closed, the mass spectrometer is vacuum-isolated from the rest of the system. The chamber separator (P), shown in Figs. 1 and 4, ensures vacuum integrity between chambers (B) and (C).

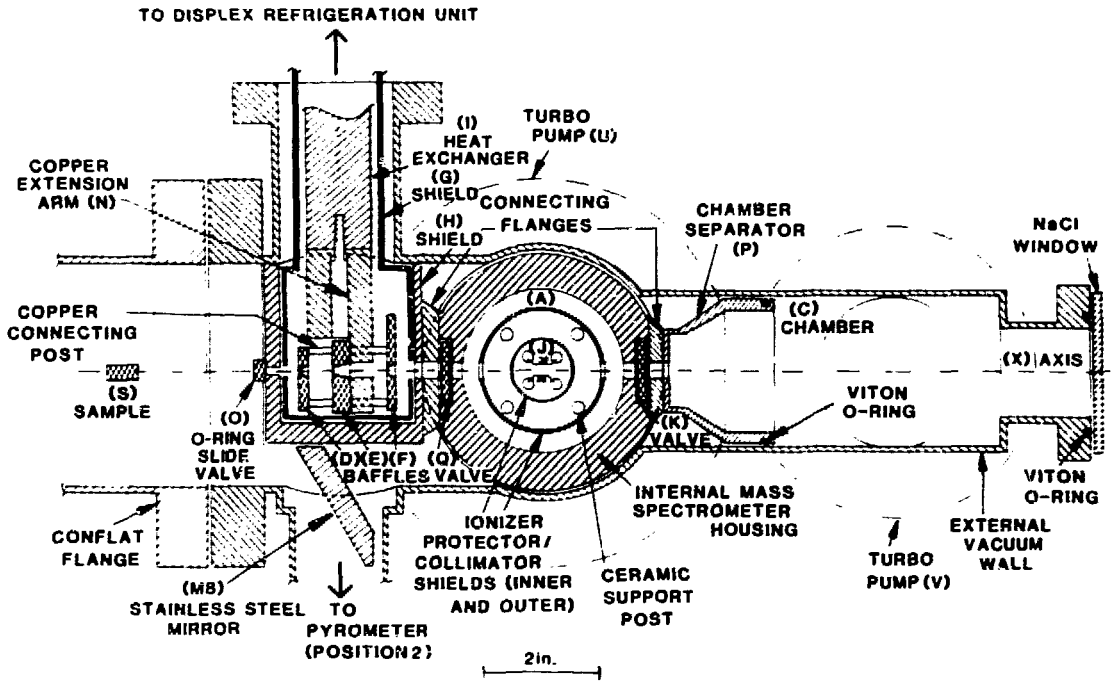

Fig. 4. Cross section of the mass spectrometer system. The plane of the diagram is perpendicular to the plane shown in Fig. 1.

D. The Cryogenic Collimation System

Figure 4 shows a diagram of the cryogenic collimating system. The plane of the diagram in Fig. 4 contains the axis (X) of the molecular beam and is perpendicular to the plane of the diagram in Fig. 1. The three copper collimating baffles (D, E, and F) are bolted and soldered (with indium solder) together. The orifice diameters in the baffles are 2 mm, 2.5 mm, and 3 mm for baffles (D), (E), and (F), respectively; these diameters define the molecular beam diameter. A nickel-plated copper shield (G) encases the three baffles. Shield (G) is then itself encased in a stainless steel shield (H), which is not in thermal contact with shield (G) or the baffles. An o-ring slide valve (O) allows the baffle system to be isolated while the main vacuum chamber (B) is open to the atmosphere. The collimating system remains at the operating temperature while samples are being loaded into the apparatus.

Baffle (E) is bolted and soldered to a copper extension arm (N), which is in turn coupled to the heat exchanger (I) of an Air Products and Chemicals, Inc., Displex Cryogenic Refrigerator. A gold/iron-chromel thermocouple is in contact with the extension arm. The shield (G) is bolted to the first stage of the cryogenic cooler. Under normal operating conditions, the baffles are held at 10 K and the shield (G) at 60 K.

E. The Laser/Furnace System

Figure 5 is a schematic of the cw, axial-discharge, CO_2 laser heating system built by the High Temperature Chemistry Group at Rice Univeristy. The glass laser tube, 2 m long and 1 cm in diameter, is encased in a water cooling jacket. Discharge leads at each end of the laser tube are normally held at 22 kV. The discharge lead in the center of the tube is held at ground potential. The back reflector mirror is gold-coated silicon (10-m focal length). The output coupler is germanium-coated (50% reflective) zinc selenide. The gas mixture is composed nominally of 61% He, 25% N_2, and 14% CO_2. During normal laser operation, the high-voltage dc power supply (Hipotronics model number 825-100) delivers 22 kV and 80 mA. The maximum available voltage and current are 25 kV and 100 mA, respectively. The beam splitter (BS) deflects 10% of the laser beam to a power meter (Scientech model number 380102). The nominal operating power is

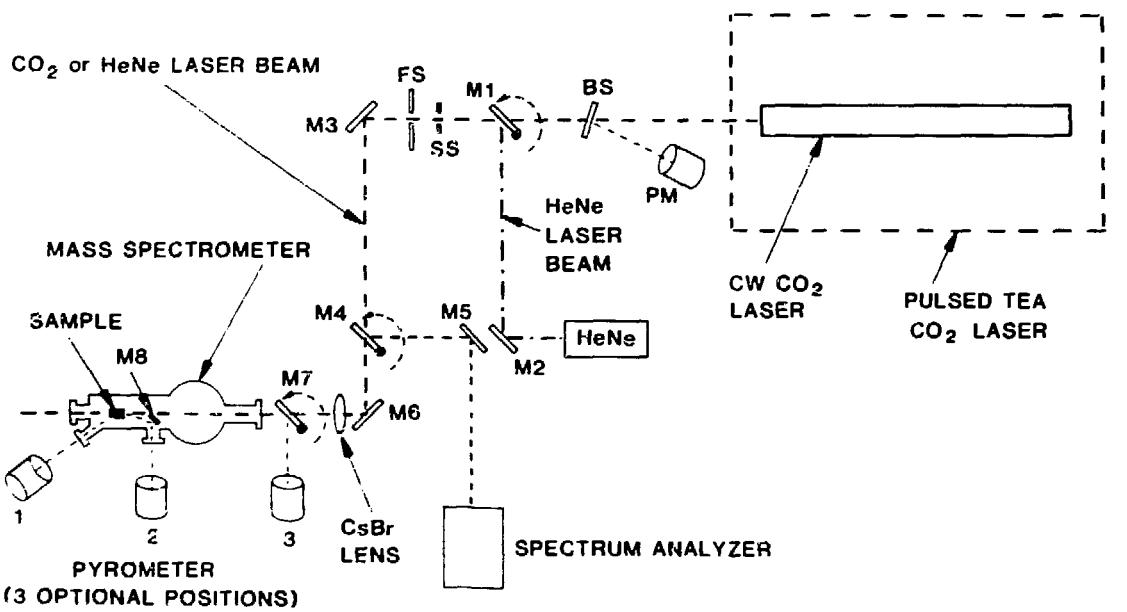

Fig. 5. The laser heating system.

100 W. The laser is optimized to the TEM_{00} mode. The cylindrically Gaussian laser beam is 1 cm in diameter at 1/e. The CO_2 laser is optimized to lase on the 00°1-10°0 [P(19)], 10.58-μm line of CO_2. The laser typically requires 10 to 15 seconds to achieve line stability after being turned on.

The dashed box in Fig. 5 indicates, as an alternative, the use of a pulsed TEA CO_2 laser (Lumonics Research, Ltd., model number K-102). The TEA laser can deliver a maximum energy of 10 J and a peak power of 33 MW. The beam divergence is 4.0 mrad. Like the cw laser, this pulsed laser uses a wavelength of 10.6 μm. Also, the optics/diagnostics system for the pulsed laser is the same as that for the cw laser.

Mirrors M1 and M2 are silver-coated glass, mirrors M3 through M7 are polished molybdenum, and mirror M8 (see Fig. 4) is polished stainless steel. Rotation of mirror M1 allows the beam from either a Metrologic 0.5-W HeNe laser or the CO_2 laser to enter the mass spectrometer. The beams of the HeNe and the CO_2 lasers are coaxial. Since the CO_2 laser light is not visible, the HeNe beam is used as an alignment guide. Rotation of mirror M4 allows the CO_2 light to enter a spectrum analyzer (Optical Engineering, Inc., model number 16-A). The spectrum analyzer monitors the wavelength of the CO_2 light as well as the line stability of the laser. A slow shutter (SS) and a fast shutter (FS) act in tandem to start and stop laser impingement on the sample. The temporal resolution of the shutter system is 1 ms. Mirrors M3 and M6 deflect the CO_2 (or HeNe) laser light to the mass spectrometer. A CsBr lens with a 50-cm focal length focuses the light onto the sample. The lens is positioned so that the sample is near the focal point of the lens, and the beam diameter at the sample is typically 1 mm.

Figure 6 shows a cross section of the resistively heated furnace. Water-cooled copper electrodes provide current to the cylindrical, 0.001-in.-thick tantalum foil resistor. An OMEGA tungsten (5% rhenium)-tungsten (26% rhenium) thermocouple, introduced through the back of the furnace, extends down the axis to within 4 cm of the mouth of the furnace. The axis of the furnace is collinear with the axis of the cryogenic baffle system. Either a sample cup or a Knudsen cell, machined from high-density graphite or molybdenum depending upon the circumstances of the experiment, is slipped onto the end of the thermocouple.

A single-color micro-optical pyrometer (Pyrometer Instrument Co., Inc.) measures the sample temperature. Figure 5 shows three optional pyrometer positions: Position 1 for laser and/or furnace heating, Position 2 only for furnace heating, and Position 3 only for laser heating when sample back-surface temperature measurements are desired. The furnace is capable of attaining temperatures of approximately 2500 K.

Figure 7 shows a third sample mounting option, which is used with laser heating. A rotating wheel (7.5 cm in diameter) holds six variable-position ring mounts as shown in the figure. As shown in Fig. 8, a ring (1 cm in diameter) holds the sample in position with tungsten wire pins, which are 0.001 in. in diameter. The rings holding the samples are slipped into the circular slots in the ring mounts. A set screw holds the sample ring in position. A set of coupled magnets allows the sample wheel to be rotated from outside the vacuum system. When a sample is rotated into the desired position, it is coaxial with the cryogenic collimating baffles and the laser beam. This mounting scheme is used for two

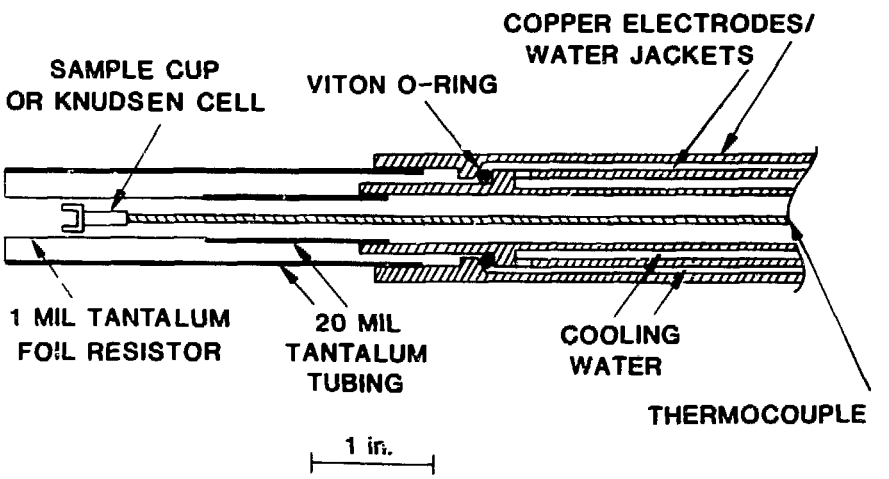

Fig. 6. Cross section of the water-cooled, resistively heated furnace.

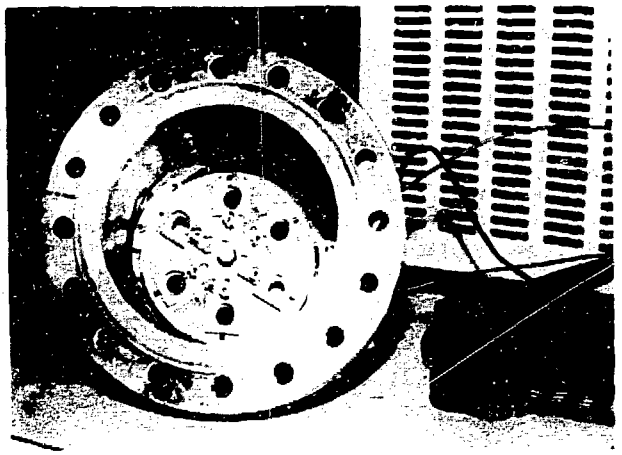

Fig. 7. The sample chamber containing the six-position sample wheel for multiple laser-heating experiments.

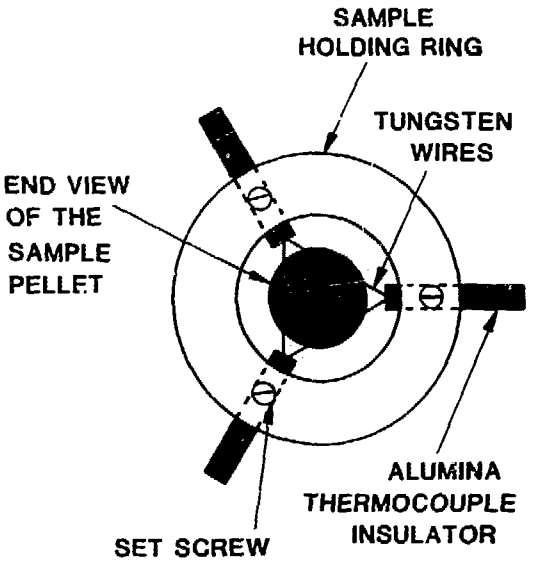

Fig. 8. The sample holding ring. The ring is slipped into one of the ring mount slots attached to the sample wheel shown in Fig. 7.

reasons. First, the tungsten wires, which have a total thermal conductivity of only about 2 W at 3000 K, are the only part of the mount in thermal contact with the sample; therefore, for all practical purposes, the only thermal loss from a heated sample is by radiation. Second, up to six samples can be studied without opening the vacuum system.

IV. MASS SPECTROMETER CALIBRATION

We used a standard mixture of hydrogen (H_2), helium, argon, krypton, and xenon to calibrate the mass scale and the quadrupole/detector mass sensitivity. Table I gives the amount (in volume percent) of each component in the gas mixture, the fractional abundances (FA) of the major isotopes, and the relative ionization cross sections (Q_i) of the major isotopes at 70 eV. We used the data in Table I to calculate the expected intensities of the major isotopes. Table II presents these intensities as expected absolute intensities (EAI) and as percentages (ERI) relative to the most abundant species (argon). For comparison, Table II also gives the observed percentages (ORI) relative to the most abundant species. As is evident from these data, the detection sensitivity may be strongly dependent upon mass. By appropriate

TABLE I. Gas Mixture for a Typical Mass Spectrometer Calibration

Element	Mass of Most Abundant Isotope (amu)	Amount in Gas Mixture (vol%)	Fractional Abundance[6]	Relative Ionization Cross Section (Q_i) at 70 eV[7]
H_2	2	33.33	0.9999	1.01
He	4	25.00	1.000	0.38
Ar	40	20.03	0.996	3.52
Kr	84	13.30	0.569	5.29
Xe	132	8.33	0.2689	7.31

TABLE II. Typical Mass Spectrometer Calibration Results

Mass of Most Abundant Isotope (amu)	EAI[a]	ERI	ORI	ERI/ORI Difference (%)
2	33.66	47.93	96.51	101
4	9.50	13.53	25.01	85
40	70.22	100.00	100.00	0
84	40.03	57.01	34.23	−40
132	16.37	23.31	7.21	−69

[a]EAI = vol% × fractional abundance × ionization cross section.

adjustment of the quadrupole control electronics, the detection sensitivity can be optimized over a selected mass range. We took the observed data from the mass spectrum shown in Fig. 9. To obtain this spectrum we used an ionization energy of 70 eV, an electron multiplier high voltage of -1.6 kV, and a scan frequency of 1 Hz. The mass spectrum in Fig. 9 is the signal average of 100 mass scans. Full-scale relative intensity corresponds to 2605 counts in the detector. The mass spectrum indicates one isotope each of hydrogen, helium, and argon, four isotopes of krypton, and seven isotopes of xenon in the mixture. Peaks at M/z = 20, 42, and ~66 result from doubly ionized argon, krypton, and xenon, respectively. Some water (M/z = 18) was present because of insufficient outgassing of the vacuum system before the calibration experiment.

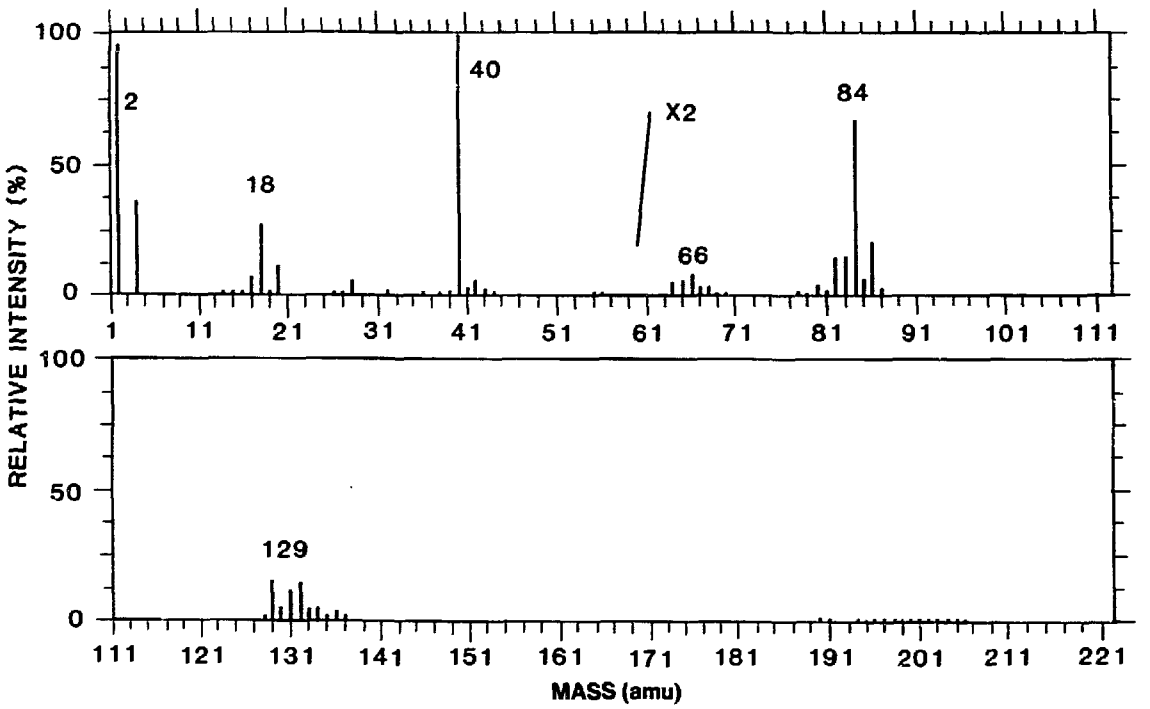

Fig. 9. Mass spectrum of a gas calibration mixture containing 33.33 vol% H_2, 25.00 vol% He, 20.03 vol% Ar, 13.30 vol% Kr, and 8.33 vol% Xe.

V. SAMPLE DATA

A. Laser Pyrolysis of Polymeric Materials

Figure 10 is the average of four mass spectral scans taken during the laser irradiation of polystyrene. Full-scale relative intensity corresponds to 1879 counts in the detector. The laser power on the sample was 7.8 kW/cm^2, the ionization energy was 70 eV, and the electron multiplier high voltage was -2 kV. We made no attempt to calibrate the mass intensities during these experiments. The most intense feature, at M/z = 104, is caused by the styrene monomer. The features at M/z = 78, 63, 51, and 26 result from fragmentation of the aromatic group. The peak at M/z = 91 could be caused by the tropilium ion, which results from rearrangement of an alkylbenzene group, or it could be caused by toluene. The tropilium ion is a common hydrocarbon fragmentation product, but fragmentation of the monomer to form toluene is also likely. Our results agree with those of Coloff and Vanderborgh.[8]

Figure 11 is the average of 11 mass spectral scans taken during the laser decomposition of polyvinyl chloride (PVC). Full scale corresponds to 2017 counts in the detector. The laser power at the sample surface was 7 kW/cm^2, and the ionization energy and the electron multiplier potential were the same as for the laser irradiation of polystyrene, described above. The lack of any mass spectral features at M/z = 62, or at any integral multiple thereof, indicates that PVC does not decompose into small chains of monomer units. Rather, the polymer decomposes first by losing HCl. The resulting molecule then fragments and forms linear and cyclic unsaturated hydrocarbons. The features above M/z = 110 are caused by vaporization of the plasticizer. These results agree with those of Lum.[9,10]

Figure 12 is the average of six mass spectral scans taken during the laser-induced decomposition of polypropylene. Full scale corresponds to 2516 counts in the detector. The laser power at the sample surface was 8 kW/cm^2, and the ionization energy and the electron multiplier high voltage were as previously stated. The features at M/z = 42, 84, and 126 show clearly that one mode of polypropylene decomposition is the removal of integral multiples of the monomer unit from the polymer. The peaks at M/z = 111, 97, 70, 55, 41, and 27 are caused by fragmentation of the various multiples of the monomer unit.

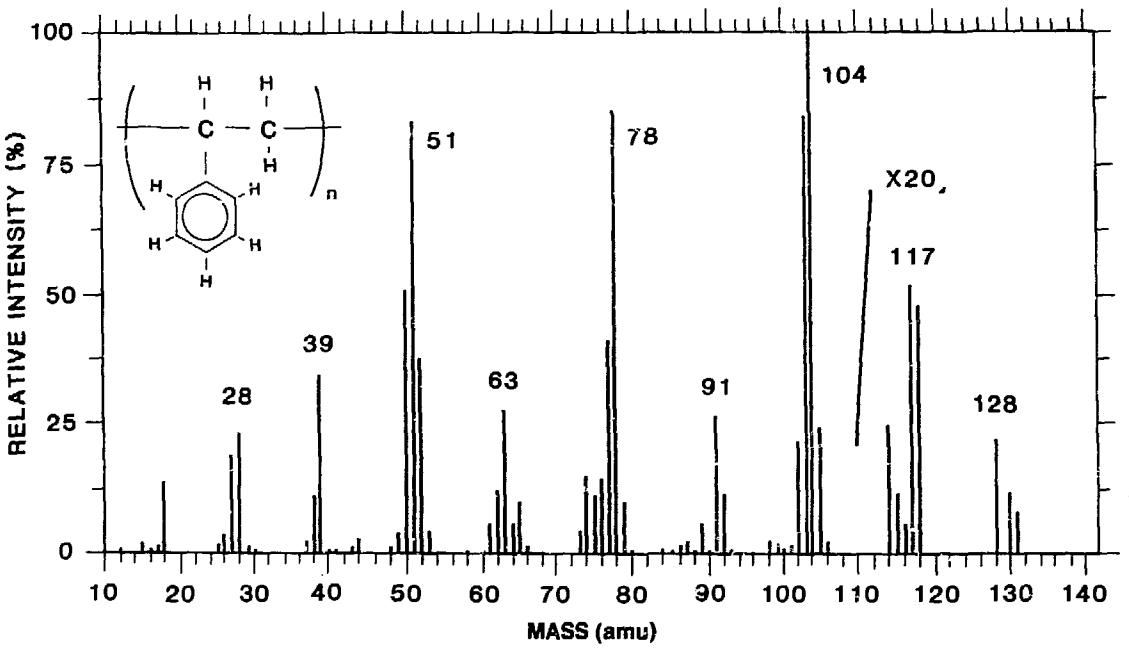

Fig. 10. Mass spectrum taken during the laser pyrolysis of commercial polystyrene.

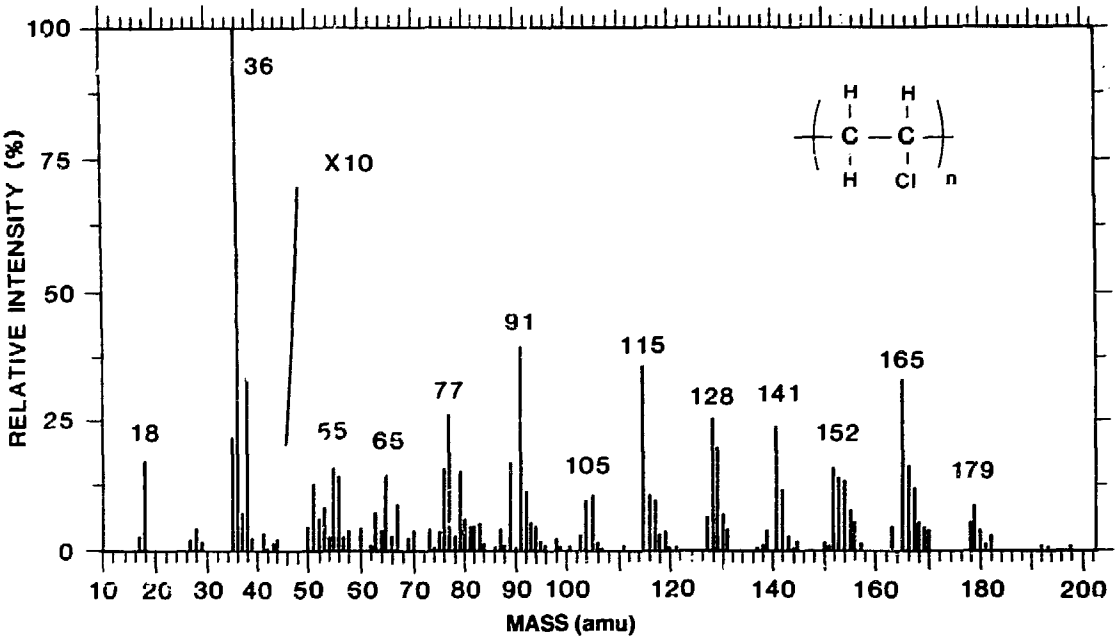

Fig. 11. Mass spectrum taken during the laser pyrolysis of commercial polyvinyl chloride.

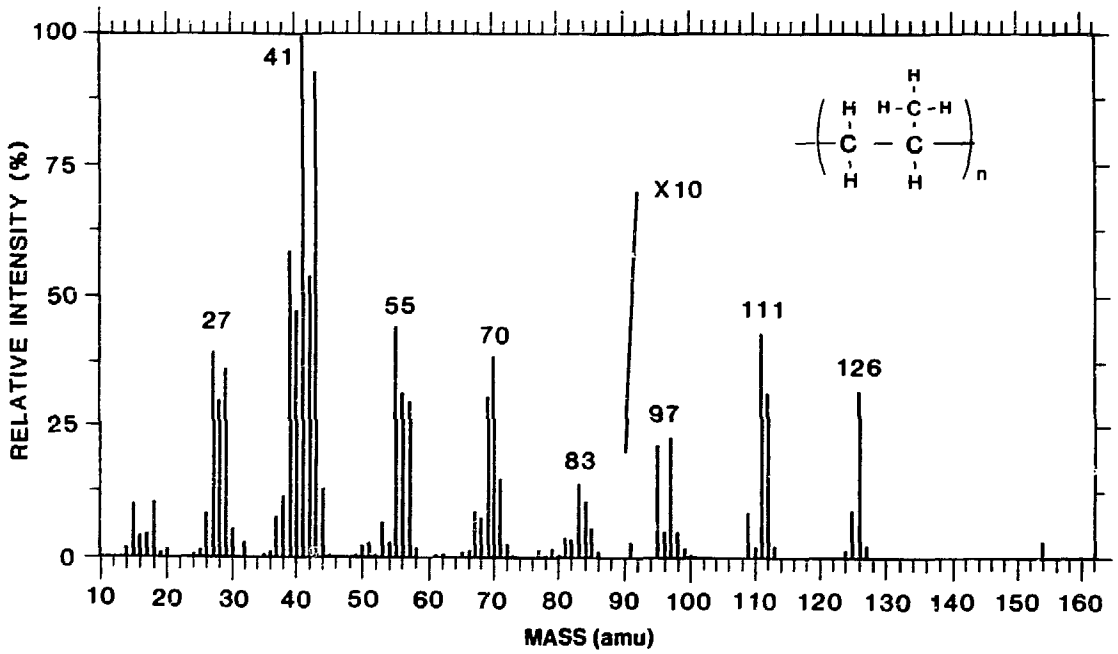

Fig. 12. Mass spectrum taken during the laser pyrolysis of commercial polypropylene.

B. Laser Vaporization of Graphite

Figure 13 is the average of 65 mass spectral scans taken during the laser-induced vaporization of high-density polycrystalline graphite. Full scale corresponds to 132 counts in the detector. The laser power at the sample surface was 7 kW/cm^2, the electron multiplier high voltage was -1.7 kV, and the ionization energy was 70 eV. With the pyrometer in Position 2, the sample temperature at the laser spot was determined to be 2300°C. Relative intensities of the peaks caused by C, C_2, and C_3 agree with the results of earlier studies.[11,12] The molecules H_2O and CO_2 are common adsorbed impurities in graphite. The molecules CO and H_2 are products of the reaction of water with the heated graphite surface.

C. Laser-Induced Combustion Synthesis

The condensed-phase combustion reaction of Ti + C is highly exothermic (reaction temperature = 3200 K). A variety of resistive heating designs as well as medium-power laser irradiation will ignite the combustion reaction. At the reaction temperature, the mass spectrometer monitors the vaporization of reagents and adsorbed impurities as a function of time. Important questions about such reactions include the following: 1) What role do adsorbed gases play in limiting the achievement of maximum theoretical density in the product? 2) Does the combustion reaction process occur under equilibrium conditions? A factor that limits product densification is the degree of impurity volatilization and outgassing during the combustion reaction. In the extreme, severe outgassing can actually blow the reacting charge apart. If the reactions occur under equilibrium conditions, then standard high-temperature thermodynamic techniques may be applied to study the reaction chemistry.

Equilibrium thermodynamic calculations indicate that the predominant gas phase species in equilibrium with TiC + C should be Ti, C, C_2, and C_3, with the equilibrium partial pressures of the latter three species being at most an order of magnitude smaller than the first. Formation of carbon monoxide results from the presence of an oxygen impurity, but its equilibrium partial pressure is proportional to the amount of oxygen impurity present in the initial charge. Figure 14 shows the time-resolved volatilization of selected vapor species during the preliminary outgassing and subsequent ignition of the reaction between Ti + C. The multiplier voltage was set at -1.8 kV, the emission current at

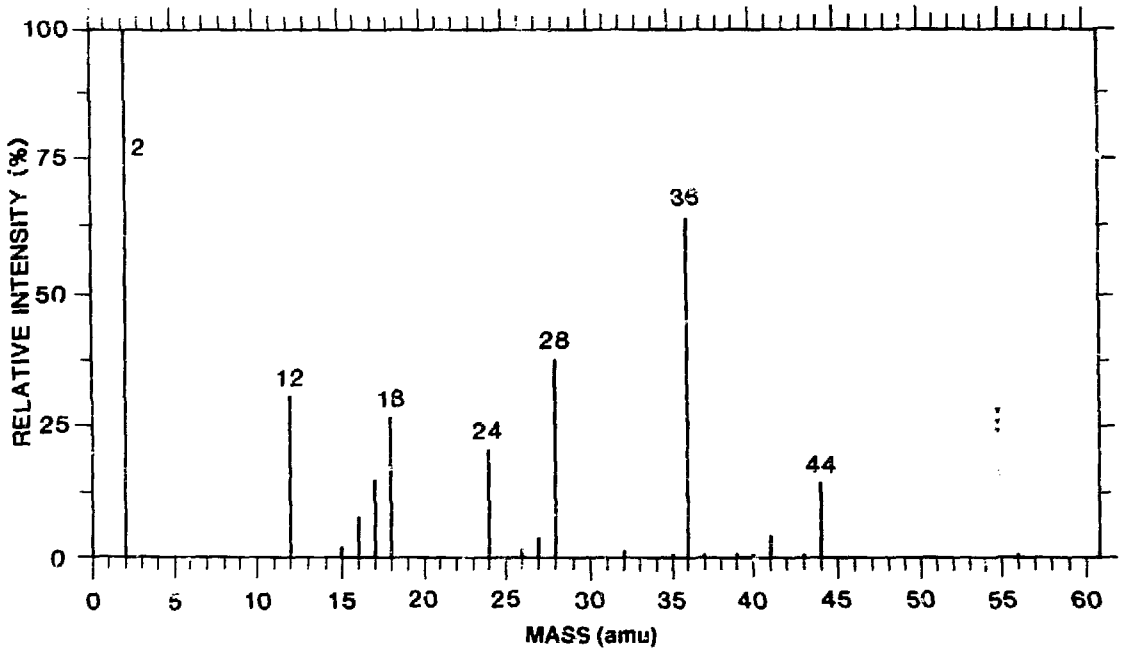

Fig. 13. Mass spectrum taken during the laser vaporization of high-density polycrystalline graphite.

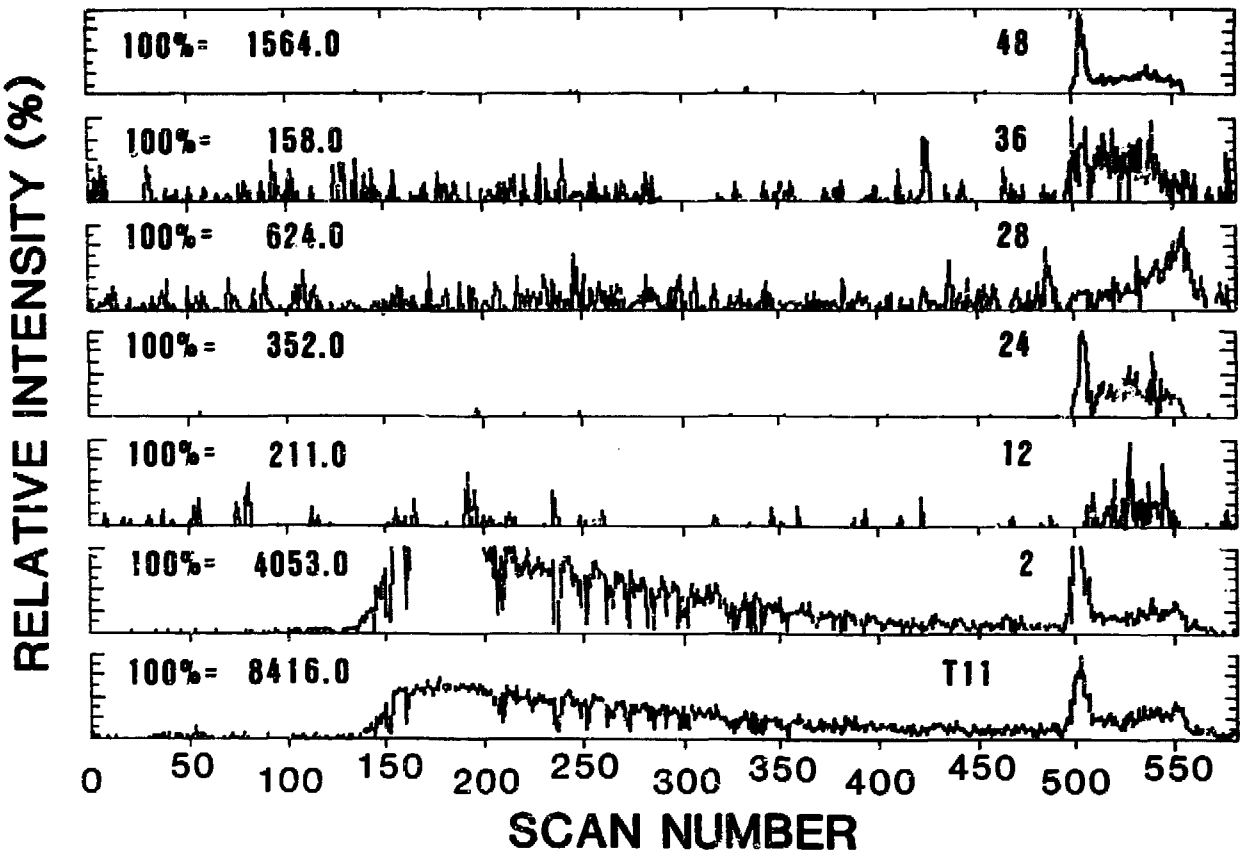

Fig. 14. Time-resolved mass spectral intensity traces of representative ion species observed during the laser-induced ignition and combustion of a compacted titanium/carbon powder mixture.

2 mA, and the ionization energy at 70 eV. The scan frequency was 2 Hz. Initially, the laser was set to operate at an output level of 10 W (1 kW/cm^2 on the sample surface). The laser shutter (SS in Fig. 5) was opened at scan number 160 of Fig. 14. Outgassing of the sample was continued until scan number 480. At scan 480 the laser power was increased to 60 W (6 kW/cm^2 on the sample surface). Ignition occurred at scan 502.

Figure 15 shows the average of scans 500 to 510. The mass spectrum has been normalized to the peak at M/z = 48 so that full scale represents 662 counts. The peak caused by H_2 is off the scale at this level of sensitivity. The pattern of peaks clustering around 48 correlates with the isotopic distribution of titanium. Very little C_2 is observable, but the peak at 36 indicates the presence of a substantial amount of C_3. The similarity of the traces for M/z = 24 and 48 in Fig. 14 indicates that Ti^{++} is the primary cause of the peak at 24 in Fig. 15. Some of the intensity at M/z = 24 could be caused by C_2, but further experiments at lower ionization energy are necessary to confirm this.

VI. SUMMARY

To evaluate the effectiveness of mass spectrometry techniques in studying vaporization from selected materials, we designed a mass spectrometer that can be used either with a cw or pulsed laser heating system or with a conventional furnace heating system. Our experimental apparatus consisted of a quadrupole mass spectrometer positioned in a crossed-beam configuration, controlling electronics, a data acquisition system, a vacuum system, a cryogenic collima-

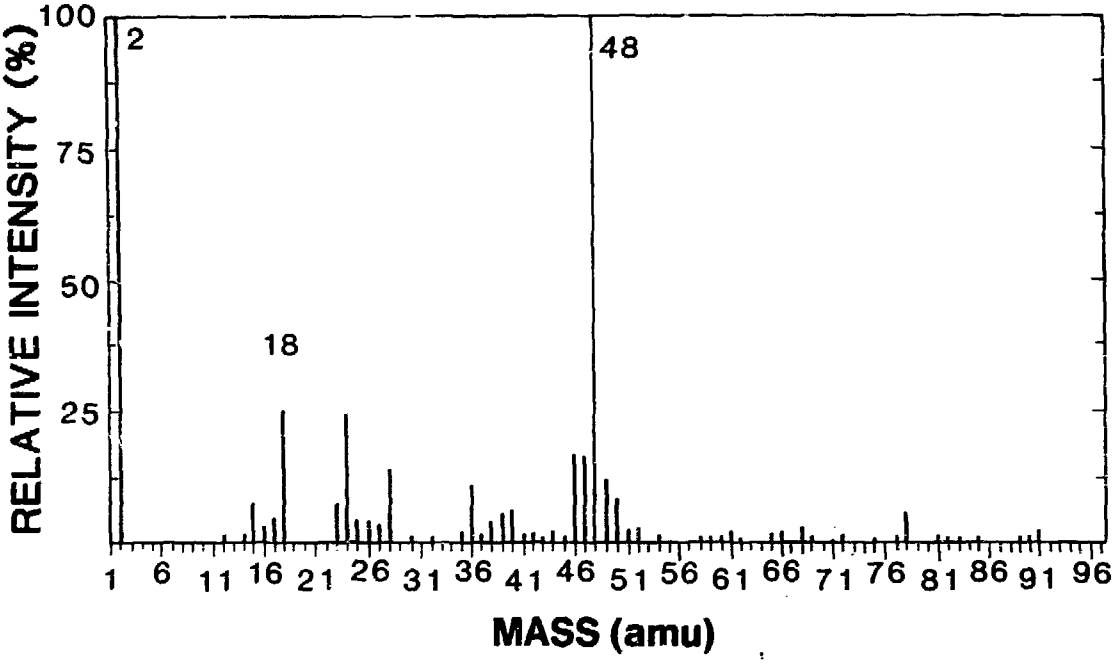

Fig. 15. Mass spectrum taken during the laser-induced ignition of a compacted titanium/carbon powder mixture.

tion system, and a laser (or furnace) heating system. We used a standard mixture of hydrogen, helium, argon, krypton, and xenon to calibrate the mass scale and the quadrupole/detector mass sensitivity.

We took several series of mass spectral scans to study pyrolysis of polymeric materials. Scans taken during the laser irradiation of polystyrene indicated monomeric fragmentation consistent with that found in other studies. Scans taken during the laser decomposition of polyvinyl chloride indicated molecular rather than monomeric fragmentation, also consistent with findings of other studies. Scans taken during the laser-induced decomposition of polypropylene showed that decomposition occurs as integral multiples of the monomer unit are removed from the polymer and further that fragmentation of the various multiples of the monomer unit also occurs.

Results of mass spectral scans taken during the laser-induced vaporization of high-density polycrystalline graphite indicate peak intensities consistent with those found in other studies. Experiments to study laser-induced combustion synthesis of Ti + C pressed-powder pellets used the mass spectrometer to monitor the vaporization of the elemental components and adsorbed impurities as a function of time during laser heat-up to ignition.

This mass spectrometer/laser system yielded excellent vaporization data for the materials examined.

REFERENCES

1. R. J. Conzemius and J. M. Capellen, "A Review of the Applications to Solids of the Laser Ion Source in Mass Spectrometry," Int. J. Mass Spectr. Ion Phys. **34**, 107-217 (1980).

2. J. Haverkamp and P. G. Kistemaker, "Recent Developments in Pyrolysis Mass Spectrometry," Int. J. Mass Spectr. Ion Phys. **45**, 275-292 (1982).

3. F. Hillenkamp, "Laser Desorption Techniques of Nonvolatile Organic Substances," Int. J. Mass Spectr. Ion Phys. **45**, 305-313 (1982).

4. R. Stoll and F. W. Rollgen, "Laser Desorption Mass Spectrometry of Thermally Labile Compounds Using a Continuous Wave CO_2 Laser," Org. Mass Spectr. **14**, 642 (1979).

5. G. J. Q. Van der Peyl, K. Isa, J. Haverkamp, and P.G. Kistemaker, "Gas Phase Ion/Molecule Reactions in Laser Desorption Mass Spectrometry," Org. Mass Spectr. **16**, 416 (1981).

6. R. W. Kiser, "A Table of Nuclide Masses and Isotopic Abundances," University of Kentucky Mass Spectrometry Center, Lexington, Kentucky (1983).

7. R. W. Kiser, *Introduction to Mass Spectrometry and Its Applications* (Prentice-Hall, Englewood Cliffs, New Jersey, 1965), p. 300.

8. S. G. Coloff and N. E. Vanderborgh, "Time-Resolved Laser-Induced Degradation of Polystyrene," Anal. Chem. **45**, 1507 (1973).

9. R. M. Lum, "Laser-Induced Decomposition of PVC," J. Appl. Polym. Sci. **20**, 1635-1649 (1976).

10. R. M. Lum, "Antimony Oxide-PVC Synergism: Laser Pyrolysis Studies of the Interaction Mechanism," J. Polym. Sci., Polym. Chem. Ed. **15**, 489-497 (1977).

11. J. Berkowitz and W. A. Chupka, "Mass Spectrometric Study of Vapor Ejected from Graphite and Other Solids by Focused Laser Beams," J. Chem. Phys. **40**, 2735-2736 (1964).

12. K. A. Lincoln, "Mass Spectrometric Studies Applied to Laser-Induced Vaporization of Polymeric Materials," *Proceedings of the Third International Symposium on High Temperature Technology* (Butterworths, London, 1969), pp. 323-332.